Catalysis Today 202 (2013) 120–127

Contents lists available at SciVerse ScienceDirect

Catalysis Today

journal homepage: www.elsevier.com/locate/cattod

Electronic changes at the Pt(1 1 1) interface induced by the adsorption of OH species

M.D. Arce[c], P. Quaino[c], E. Santos[a,b,*]

[a] Faculdad de Matemática, Astronomía y Física, Instituto de Física Enrique Gaviola (IFEG-CONICET), Universidad Nacional de Córdoba, 5000 Córdoba, Argentina
[b] Institute of Theoretical Chemistry, Ulm University, D-89069 Ulm, Germany
[c] PRELINE – Fac. Ing. Química – UNL, 3000 Santa Fe, Argentina

ARTICLE INFO

Article history:
Received 5 December 2011
Received in revised form 14 April 2012
Accepted 18 April 2012
Available online 13 June 2012

Keywords:
Hydroxyl
Platinum
Density functional calculations
Density of states
Chemisorption

ABSTRACT

We perform a detailed analysis of the modifications in the electronic properties when an OH radical adsorbs on Pt(1 1 1). On the basis of first principle calculations, we provide an overview of the interface at the atomic level at low coverages (1/9 of a monolayer). The electronic factors that govern the adsorption phenomenon are discussed. The interaction of the electronic states involved in the bond formation is investigated. In this context, we examine the charge redistribution and the projected density of states onto the different participating atoms and orbitals. We establish a comprehensive picture which provides a valuable guideline to understand the complicated interplay of the electronic states in the formation of bonds.

© 2012 Elsevier B.V. All rights reserved.

1. Introduction

The adsorption of OH species plays an important role in various catalytic, electrocatalytic and photocatalytic reactions, such as oxygen reduction and water splitting [1,2]. Also, OH_{ads} is the oxidant of CO(ads), the troublesome poison of anodes in fuel cells and alcohol oxidation [3]. Understanding the electronic interactions between adsorbed species and substrate is crucial to develop new catalysts [4]. Consequently, the adsorption of oxygen, hydroxyl and water species on different substrates has been extensively investigated, both theoretically and experimentally (see for example, [5–10]). Since the pioneering work of Fisher and Sexton [11], who first demonstrated by a combination of spectroscopies that in the presence of adsorbed atomic oxygen, water dissociates to form adsorbed hydroxyl species, diverse experimental and theoretical approaches have been used to elucidate the binding mechanism and the structure of the OH overlayer on a metal surface. Particularly interesting is the subtle balance between water–water hydrogen bonding and water–substrate interactions, which governs the formation of adsorbates structures [12]. Calculations using density functional theory (DFT) [7] have shown that at low coverages (1/9 to 1/3 of a monolayer) hydroxyl adsorbs preferentially at bridge and top sites. However, due to the lower diffusion barrier of isolated OH and the tendency to form H bonds between neighbouring OH groups, hydroxyls are susceptible to island formation also at low coverage. At higher coverages, lateral interactions through H bonding causes the formation of OH networks. These authors suggested that the intermediate in water formation consists of a mixed $OH + H_2O$ overlayer. Diverse structures of water–hydroxyl have been proposed and carefully investigated [6,10,13–15]. It has also been shown that long range Coulomb interactions in oxygen superstructure formation play an important role at higher coverages [16].

These processes still seem to be more complicated in electrochemical systems, as revealed by Koper [17]. He has analyzed the response of different electrode metals in a wide potential region and found anomalous behaviour involving replacement process, and formation of OH_{ads} at potential region where only hydrogen usually adsorbs.

Recent results [12] reveal that the simple, conventional ice 'bilayer' description of water adsorption, which is frequently used for theoretical calculation in electrochemical environment [18], is inadequate.

Frequently, DFT calculations are performed focusing on the energetics of the system, and empirical correlations are employed to predict reactivity. Less attention is paid to the electronics, with some exceptions [8,13,19–21]. It is to notice that specially in the present system, where the interaction between the adsorbed

* Corresponding author at: Faculdad de Matemática, Astronomía y Física, Instituto de Física Enrique Gaviola (IFEG-CONICET), Universidad Nacional de Córdoba, 5000 Córdoba, Argentina.
E-mail address: esantos@uni-ulm.de (E. Santos).

0920-5861/$ – see front matter © 2012 Elsevier B.V. All rights reserved.
http://dx.doi.org/10.1016/j.cattod.2012.04.062

species is very important, most of the functionals used in DFT calculations do not properly account for hydrogen bonding within water structures [22,23]. Also cations markedly affect the adsorption of OH through a weakening of the repulsive interactions between the OH in the OH adlayer [24].

Thus, a challenge for theoreticians is to propose realistic models to understand the processes occurring in an electrochemical environment.

Since the electronic participating in the bonds shows a complicated interplay, an analysis only based on frontier orbitals is not adequate for a quantitative description. Recently [20], it has been shown that the adsorption of OH at platinum substrates does not follow the d-band model developed by Hammer and Nørskov [25]. This anomalous behaviour has been attributed to the repulsive interaction of the substrate d-band with the renormalized adsorbate states.

In this work, we shall explore the modification of the electronic properties of the substrate induced by the adsorption of hydroxyl. We shall limit our analysis to low coverages of the OH species and focus on the density of states projected onto the different atoms. One of the goals is to obtain the orbital composition of the resulting bonds between platinum and hydroxyl. The combination between the analysis of modification of the work function, charge rearrangements, interfacial potential redistribution and population of the different electronic states provide a consistent picture and a deeper insight into the factor governing the adsorption process. This analysis is essential to perform *quantitative* studies and to abandon *qualitative* analysis only based on *empirical* correlations. The development of the theoretical tools today allows us to go this step forward. The detailed study of the electronic interaction presented here is a prerequisite for calculating the kinetics of the adsorption process, which involves the knowledge of the interaction constants. We need to know precisely which orbitals are participating in the adsorption process. All these data can be used to apply the theory of electrocatalysis proposed by us in previous publications [26–28] and calculate kinetic parameters in an electrochemical environment.

2. Computational details

2.1. First principles calculations

All calculations were performed using the DACAPO code [29]. This utilizes an iterative scheme to solve the Kohn–Sham equations of density-functional theory self-consistently. A plane-wave basis set is used to expand the electronic wavefunctions, and the inner electrons were represented by ultrasoft pseudopotentials [30], which allow the use of a low-energy cut-off for the plane-wave basis set. An energy cut-off of 450 eV was used in the calculations. The electron–electron exchange and correlation interactions are treated with the generalized gradient approximation in the version of Perdew et al. [31]. The Brillouin-zone integration was performed using a $4 \times 4 \times 1$ k-point Monkhorst–Pack grid [32] corresponding to the 1×1 surface unit cell. The energy accuracy was reached when the change in the absolute energy value was less than 10 meV. For relaxations, the convergence criterion was achieved when the total forces were less than 0.02 eV/Å. Unless mentioned spin-polarization was not considered. Dipole correction was used to avoid slab–slab interactions [33]. The molecular graphics have been done with the XCRYSDEN package [34].

2.2. Slab modelling

The behaviour of OH radical on Pt(1 1 1) surface has been investigated. The surface was modelled by a (3×3) supercell with 4 metal layers. In all the calculations 8 layers of vacuum were considered. For the relaxations, the two bottom layers were fixed at the calculated next-neighbour distance corresponding to bulk, and all the other layers were allowed to relax. The optimized surface – prerelaxed Pt(1 1 1) – in the absence of OH were used as input data to carry out the calculations.

For the adsorption to take place, the OH radical was located on a top site of the bare Pt(1 1 1) according to site stabilities. A coverage of 1/9 was considered in all the calculations. Less OH–Pt coordination and larger OH–metal distances minimize the repulsive interaction and favour the adsorption process given the following adsorption energies: (1) top (−2.62 eV), (2) bridge (−2.57 eV), (3) hollow (−2.17 eV hcp, −2.28 eV fcc) in agreement with values of the literature [6,7,35]. The pre-relaxed surfaces were kept fixed while the H in OH radical was fully relaxed. The O was frozen in all the coordinates at different *z*-distances perpendicular to the surface. The optimized geometry at final equilibrium (OH_{ads} almost flat parallel to the surface) is also in accordance with literature data [21].

3. Results and discussion

3.1. Electronic charge rearrangement at the interface Pt(1 1 1)/OH

The goal of this contribution is not to discuss the energetics or the geometry of the adsorbate, because these aspects have been already investigated by other authors and are well established. Here, we shall analyze the modification in the electronic structure of platinum when a layer of hydroxyl is adsorbed on the (1 1 1) surface at 1/9 coverage. Our aim is to understand the electronic interaction between OH and the platinum surface as a first step before to go forward and investigate the more realistic situation of mixed layers of $OH–H_2O$.

As pointed out in [36–38], the electronic changes produced in the substrate originate from two effects: the dipole of the species to be adsorbed and an interfacial dipole resulting from both the change of the intrinsic surface dipole and the redistribution of charge caused by the bond formation between adsorbate and metal surface.

In order to evaluate the contribution of the different components of the interface, we shall proceed as follows: first, the situation of the *isolated* layer of OH species will be investigated. The OH radicals are considered in the geometry they will take on upon adsorption at the Pt(1 1 1) surface. We have to stress that this 2D layer is different from that of the single OH species because of the alignment of their individual dipole moments. At the bottom of Fig. 1, the plane-averaged potential of this layer and the corresponding density of states projected onto the oxygen and hydrogen atoms are shown. The sp- and d-states projected onto the platinum surface atoms in the *absence* of adsorbates are also included. In the potential profiles, we can distinguish two regions where the macroscopic electrostatic potential in the vacuum has different values. In this case, the difference between the left and the right sides is −0.263 eV. In principle, if we do not consider the mutual depolarization of the species, this nominal potential jump ΔE_{vac} across the dipolar layer of hydroxyls is related to the projection of the molecular dipole moment onto the surface normal $\mu_{\perp}$, through the Helmholtz equation:

$$\Delta E_{vac} = -\frac{\mu_{\perp}}{\varepsilon_o A} \quad (1)$$

where A is the area of the unit cell and ε_o is the vacuum permittivity.

Because OH is a radical, spin polarization produces the split of the molecular states. The molecular states 3σ shows two peaks at −4.0 eV (spin up) and −4.7 eV (spin down), where an overlap of states of hydrogen and oxygen atoms is evident. The states 1π, at

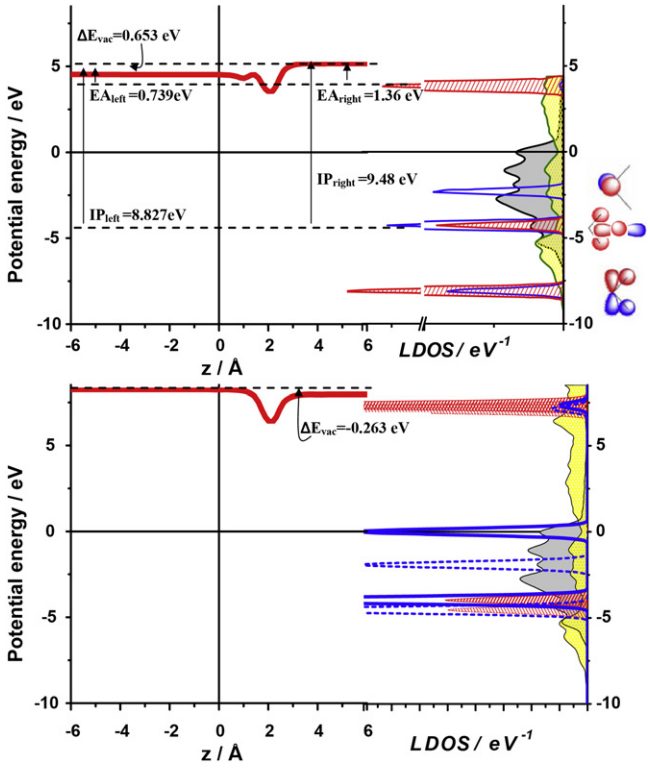

Fig. 1. Plane averaged electron potential energy profiles (on the left side) and projected density of states of the isolated components of the systems (on the right side) onto the 1s states of hydrogen atom (red dashed surface curves), total states of oxygen atom (solid (spin up) and dashed (spin down) blue line), 6sp states (yellow dashed surface curves) and 5d states (grey dashed surface curves) of platinum atom corresponding to the top position of OH. Upper plots: water isolated layer. Bottom plots: OH isolated layer. Both at the frozen position corresponding to the adsorbed layer in equilibrium. The different values for the ionization potentials (IP), electron affinity (EA) as well as the difference in the vacuum levels (ΔE_{vac}) are indicated. (For interpretation of the references to colour in this figure legend, the reader is referred to the web version of the article.)

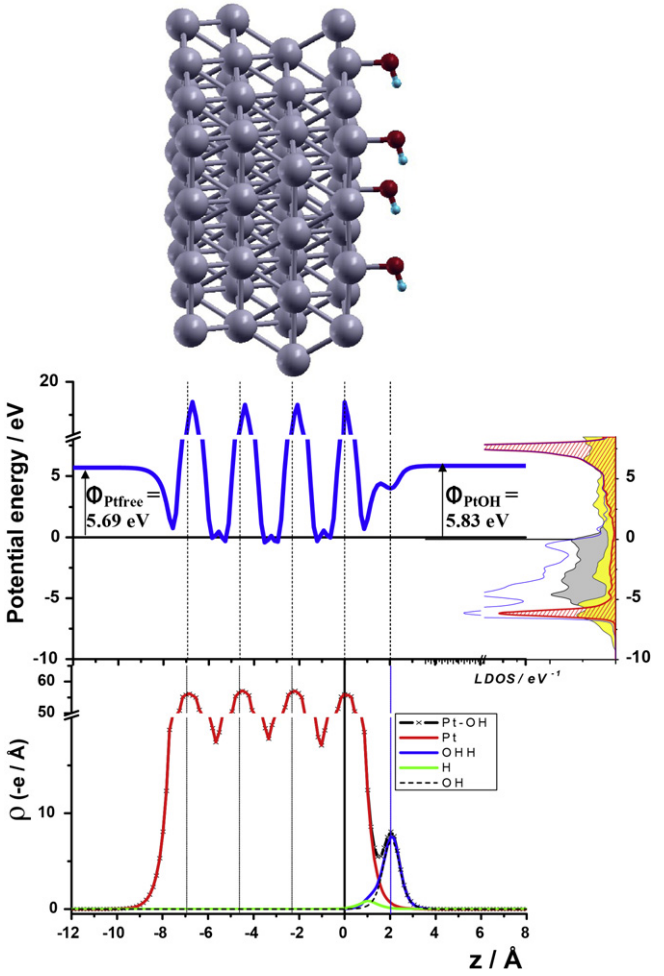

Fig. 2. Plane averaged electronic charges and potential energy profiles of the combined system adsorbed hydroxyl layer on Pt(1 1 1). The projected density of states are shown at the right (same symbols as in Fig. 1). The values of the work functions Φ_{Pt} are also indicated.

−2.0 eV correspond to the lone pair electrons, while the states half occupied (exactly at the Fermi level) correspond to the unpaired electron of the OH radical in the oxygen atom. The states $4\sigma^*$ of OH can be observed at about 7.4 eV. These features of the density of states are in accordance with previous results in the literature [20]. If the OH radical is terminated with a H atom whose position is optimized forming a water molecule, the resulting electrostatic profile and projected density of states are those shown in the upper part of Fig. 1. In this situation, the shift of the vacuum level occurs in the opposite direction and is +0.653 eV, due to the presence of the extra H at left side, which modifies the geometry of the dipole layer. In this situation, no effect of spin polarization occurs. The density of states shows three peaks below the Fermi level and one above it. The positions of these peaks are shifted to lower energies in comparison with those of the hydroxyl species. We can clearly identify the $1b_2$ (at −8.0 eV), the $3a_1$ (at −4.3 eV) and the $1b_1$ (at −2.3 eV) molecular orbitals of water. The overlap between the atomic orbitals of oxygen and hydrogen is evident for the two peaks at lower energies. The $1b_1$ state mainly corresponds to the lone electron pairs localized at one of the p orbitals of the oxygen atom.

At a second step, we analyze the behaviour of the 2D-layer in equilibrium with the Pt(1 1 1) surface. Fig. 2 shows the plane-averaged potential of the system as a function of the *z*-coordinate (perpendicular to the surface). The electronic charge distributions of the whole system (Pt–OH), the isolated surface (Pt), the isolated hydroxyl layer (OH), the isolated water layer (H–OH), and the isolated hydrogen (H) added for the saturation of the OH radical are also given. In addition, similar as in Fig. 1, the projected density of states is plotted. A broadening and a shift in the position of the different orbital contributions can be observed caused by the interaction of the adsorbate with the electronic states of the metal. Particularly noticeable is the profile of the density of states projected onto the oxygen atom: the contour follows almost the distribution of the d states of surface platinum atoms. In contrast to the results observed with an adsorbed water layer on Pt(1 1 1) [39], the changes in the electronic states of the surface atoms of platinum are also significant. We shall return to this point in the next section.

The induced modification of the Pt work function by the presence of the hydroxyl adlayer is about $\Delta\Phi_{Pt}$ = +0.14 eV. Seitsonen et al. [21] have calculated an increase of the Pt work function of about 1 eV when the surface is covered by $\sqrt{3}\times\sqrt{3}$R30°-2OH adlayer. Energy loss spectroscopy measurements for water adsorption on clean and oxygen covered Pd(1 0 0) [40] have given the following values: when the clean surface was exposed to 3 Langmuir of water, a change of −0.4 eV was measured. The authors interpreted the spectrum as that of an ice-like two dimensional water layer. When a previously covered $p(2\times2)O$ surface is exposed to 2 Langmuir of water, the change in the work function was in the opposite direction (+0.1 eV). Here some water molecules react with the pre-adsorbed oxygen atoms to form hydroxyl. By

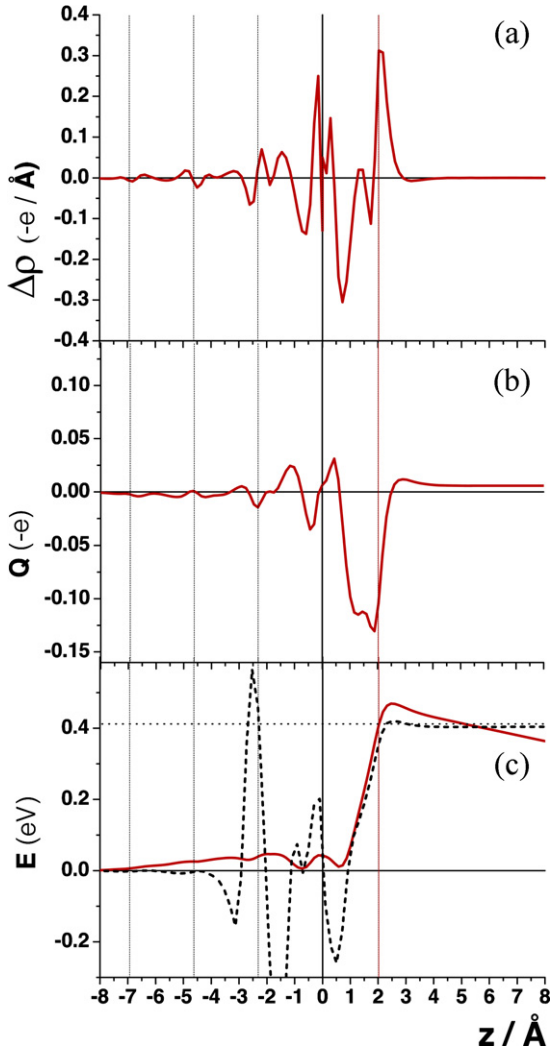

Fig. 3. Charge rearrangement $\Delta\rho$ calculated according to Eq. (2) (a), charge transfer per OH species Q calculated by integration of $\Delta\rho$ over z (b), and potential energy for the bond formation (c). The latter has been calculated by three different ways: integration of Q over z according to Eq. (4) (solid line), subtraction of the work functions and the vacuum levels according to Eq. (3) (dot line), and by the difference between the electrostatic potential energies of the whole system and the isolated metal and OH layer (dashed line).

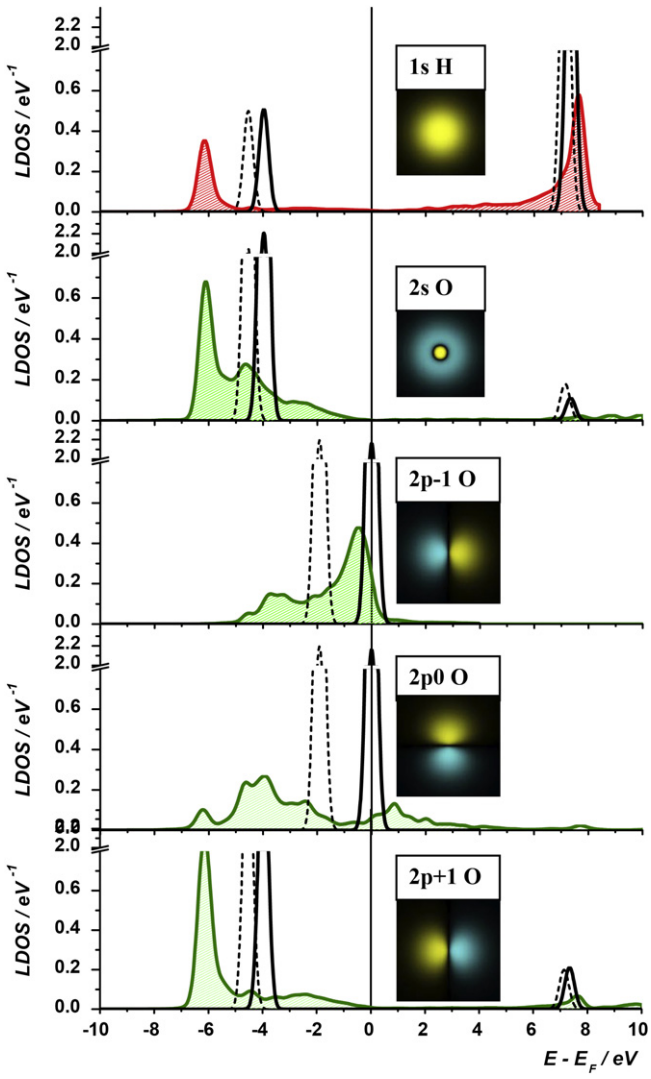

Fig. 4. Projected density of states onto the different electronic states corresponding to hydrogen and oxygen atoms for: isolated layer (black solid (spin up) and dashed (spin down) lines) and adsorbed layer (dashed surfaces).

heating at 200 K an increase of 0.35 eV in the work function was determined and the spectrum indicates that the remaining water molecules have either desorbed or reacted to form hydroxyl. Therefore our value is reasonable taken into account that the coverage is much lower than that used in [21]. This value has the opposite sign to those caused by a water layer on Pt(1 1 1), where values between −0.23 and −2.27 eV, depending on the hydrogen orientation, have been calculated [39]. Obviously, the water layer has an extra hydrogen atom which changes the orientation of the dipole. At the left, the Φ_{Pt} = 5.69 eV coincides with the value of the isolated Pt surface. These changes are produced by the dipole of the adlayer and the consequent redistribution of charges at the interface [37]. OH adsorbed acts as an electron acceptor, thus it is expected that some electron density flows from the Pt atoms towards the hydroxyl groups. We shall confirm this fact by other calculations, as we shall next discuss.

The corresponding rearrangement of electronic charge upon the formation of the adsorbed layer can be obtained by subtracting the charge densities of the non-interacting systems (isolated Pt surface ρ_{Pt}, and isolated 2D-layer of OH ρ_{OH}, both frozen at their final equilibrium configuration upon adsorption) from those where the adlayer of OH interact with the Pt(1 1 1) surface ρ_{Pt-OH}:

$$\Delta\rho = \rho_{Pt-OH} - \rho_{Pt} - \rho_{OH} \quad (2)$$

In Fig. 3a the laterally averaged charge density difference $\Delta\rho$ as a function of the position perpendicular to the surface is plotted. Firstly, the results indicate that most of the charge rearrangement occurs in between the top two Pt layers and the oxygen atom of the hydroxyl. Because of the large electronegativity of oxygen, surface electronic charge flows from the platinum to the region close to the oxygen atoms. Simultaneously, the induction of the image counter charge near the surface is clearly observed. This redistribution of charge causes an additional effective dipole layer that further increases the work function. The integral of this density charge difference along the surface normal is shown in Fig. 3b. The minimum separates the regions of excess and deficiency of charge. There is a net charge transfer from the substrate to the adsorbed layer. However, the fact that at long distances it approaches zero indicates that net charge of the whole system is maintained. Then, the overall modification of the work function resulting from covering the Pt(1 1 1) surface with a hydroxyl layer is a consequence

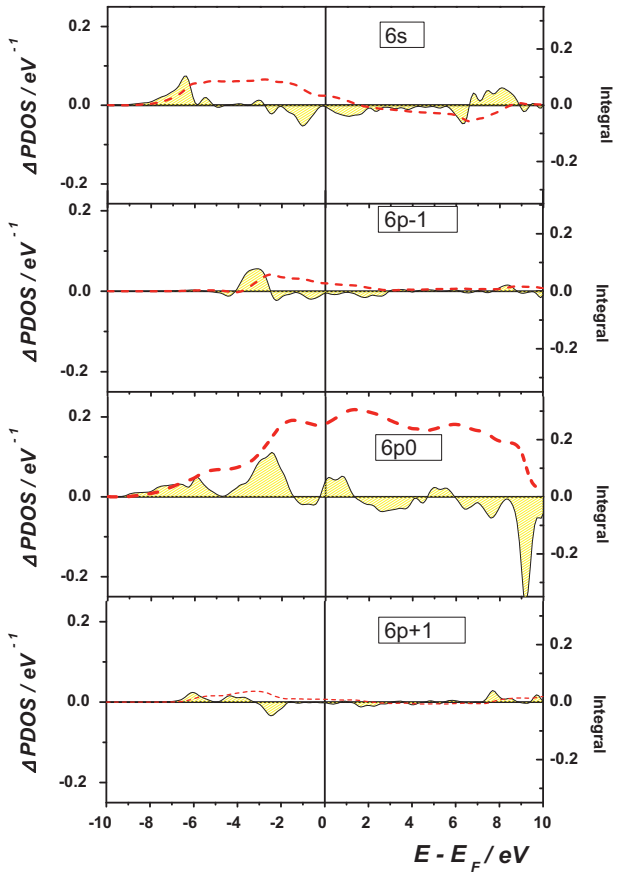

Fig. 5. Differences between the projected 6sp density of states onto the different electronic states corresponding to the platinum atom isolated and in contact with the OH species (dashed surfaces). The dashed lines correspond to the integration of the differences over the energy coordinate.

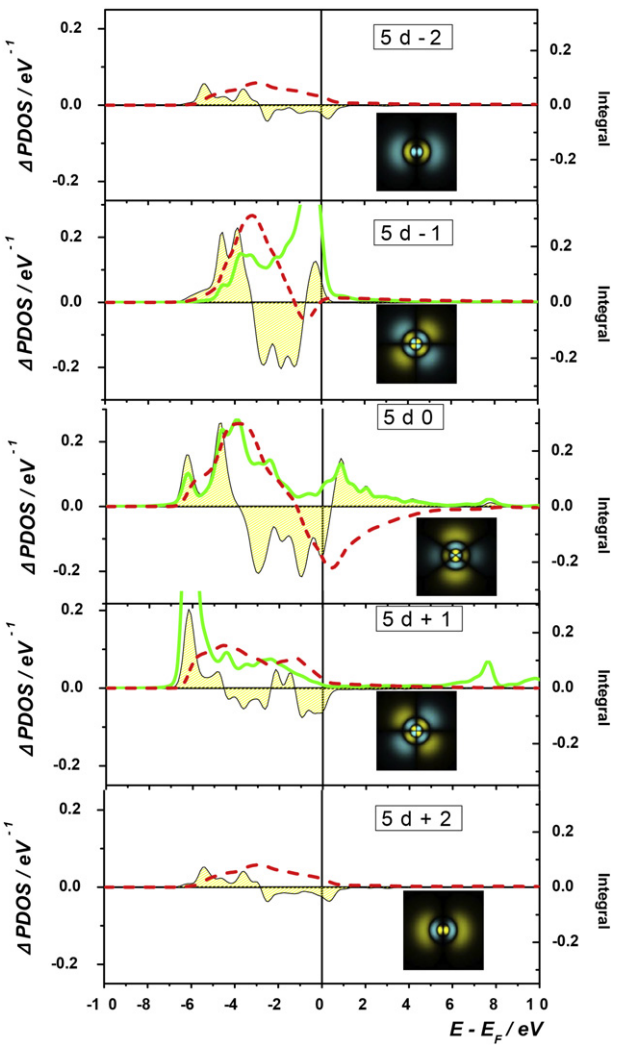

Fig. 6. Differences between the projected 5d density of states of a platinum surface atom in the absence and the presence of an adsorbed OH species (dashed surfaces). The dashed lines correspond to the integration of the differences over the energy coordinate. Also the components of the p states of the oxygen are shown (green lines). According to the symmetry conditions, the $2p_0$ states of the oxygen can overlap with the $5d_0$ of the platinum and the $2p_{\pm1}$ with the $5d_{\pm1}$. (For interpretation of the references to colour in this figure legend, the reader is referred to the web version of the article.)

of two effects: the molecular dipole moments expressed by ΔE_{vac} and the bond dipole BD defined as [37]:

$$BD = \Delta\Phi - \Delta E_{vac} \tag{3}$$

In the present system this gives the value of $BD = 0.41$ eV. This bond dipole associated with the modification of the electrostatic potential upon bond formation, can be also obtained by solving the Poisson equation:

$$\frac{d^2V_{bond}}{dz^2} = -\frac{\Delta\rho}{\varepsilon_o A} \tag{4}$$

where A is the area of the unit cell and ε_o the vacuum permittivity. The microscopic distribution of the potential energy $E_{bond} = -eV_{bond}$ is shown in Fig. 3c. The total change through the whole adsorbed layer is of the same order of magnitude as the difference between the vacuum levels and the work function calculated above (the pointed line in Fig. 3c). An additional way to corroborate this result is to perform the difference between the electrostatic potential energies of the whole system and the isolated metal and OH layer. This is indicated by the short dashed curve in Fig. 3c. Although large oscillations caused by numerical uncertainties (the subtraction of large numbers giving small numbers) are observed, the resulting value at large distances coincides with those obtained by the other two methods.

3.2. Analysis of the modifications on the projected density of states

Seitsonen et al. [21] have suggested that the bonding of OH on Pt(1 1 1) is essentially identical to that of OH to a single H atom in H_2O. They supported their view analyzing and comparing the hybridization of the orbitals of the hydroxyl with the states of a single atom and the Pt(1 1 1) (broadened with a Gaussian of width 0.35 eV) to those of water. Based in this simple feature they concluded that the hybridization of OH on Pt(1 1 1) should be sp^3. Although this analysis is qualitatively correct, the interplay between the electronic states of the metal and the adsorbate are much more complicated, as we shall next discuss.

Fig. 4 shows the density of states projected onto the 1s state of the hydrogen atom and the different states (2s, 2p−1, 2p0, 2p+1) of the oxygen atom for both the adsorbed and the isolated hydroxyl layer. The effect of spin polarization is clear for the isolated layer of OH radicals. In this case, the 3σ states have contribution of the atomic orbitals of oxygen 2s and 2p+1 which overlap very well with the 1s atomic state of hydrogen. The $2p_{-1}$ and $2p_0$ states seem

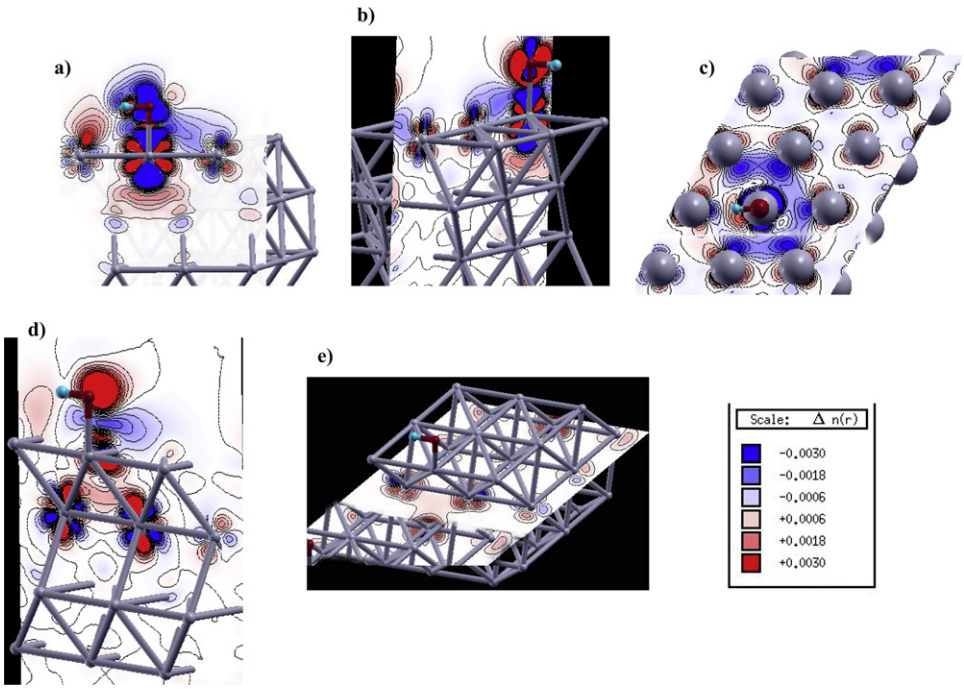

Fig. 7. Various cross sections of the charge density difference for the Pt—OH bonds. (a) Plane containing the OH axis and the central metal row where it is adsorbed. (b) Cut in the plane perpendicular to the OH bond. (c) Plane corresponding to the top layer of the platinum slab. (d) Plane parallel to the OH axis and containing the second metal row where it is adsorbed. (e) Plane corresponding to the second layer of the platinum slab next to that where the OH is adsorbed. (For interpretation of the references to colour in the text, the reader is referred to the web version of the article.)

to be partially hybridized, sharing the lone pair electrons and the unpaired electron.

The interaction with the metal surface produces a complex interplay of electronic states. The 3σ states are broadened and shifted towards lower energies with a distinct peak at −6.0 eV coincident with the 1s state of hydrogen. It is also evident a small contribution of the $2p_0$ states. A second less pronounced maximum can be observed at about −4.5 eV followed by a broad region which extends just to the Fermi level. Concerning the two p partially hybridized states at higher energies (one at −2.0 eV and another centred at the Fermi level when the OH layer is not interacting with the metal, i.e. p_{-1} and p_0 of the oxygen atom), they show distinct behaviour when the layer becomes in contact with the platinum surface. On one hand, the p_{-1} states is shifted to lower energies and split showing a pronounced maximum at about −0.4 eV and a second broader smaller peak at about −3.5 eV. On the other hand, the p_0 states of oxygen split in a small part shifted to higher energies above the Fermi level (with a maximum at +0.9 eV) and a complex structure at lower energies. The latter part shows a small peak at −6.0 eV coincident with the peak of the 1s states of hydrogen, as mentioned above. Further, a broad region between −5 and −2 eV is observed.

In order to understand the interactions of the adsorbed layer with the different electronic states of the metal, we have projected the total density of states onto the different components of the electronic states corresponding to the platinum atoms of the top position: 6s, $6p_{-1}$,$6p_0$, $6p_{+1}$; $5d_{-2}$, $5d_{-1}$, $5d_0$, $5d_{+1}$, $5d_{+2}$. Due to the complexity of the changes observed on the density distribution pattern, we shall proceed to evaluate the difference between the Pt–OH system and the bare surface Pt(1 1 1) to facilitate the interpretation and to make some relevant features visible.

Fig. 5 shows the results for the s and p states of platinum, and Fig. 6 those corresponding to the d states. The integrated differences are also shown (dashed lines). All electronic states are more or less affected by the interaction, but in particular those extending towards the perpendicular direction of the surface. It is interesting that the $6p_0$ states become more populated while the $5d_0$ appears depleted, as can be inferred from the integrated curves. Thus, the presence of the adsorbed layer induces an interband transfer of electrons. The lowest peak corresponding to the sigma molecular orbital of the hydroxyls (at about −6.0 eV) overlaps with those peaks related to the increase of population of the 6s, $6p_0$, $5d_0$ and $5d_{+1}$ states of the platinum atoms. The two regions of the $2p_{-1}$ states of the oxygen coincide with the pattern of electronic redistribution of the $5d_{-1}$ states of the metal, indicating the formation of bonding and antibonding π orbitals, the latter lying below the Fermi level. Stronger σ bonding and antibonding states are evident from the comparison of the $2p_0$ states of oxygen with the $5d_0$ states of the metal. Here, a very close correspondence between the $2p_0$ electronic states of the adsorbate and the changes of the $5d_0$ is observed (see Fig. 6). Since in this case, the region corresponding to the antibonding states lies above the Fermi level, the bond is stabilized. In the intermediate region between these states, the electronic density decreases in the $5d_0$ and $5d_{-1}$and simultaneously increases in the $6p_0$ states of the metal.

3.3. Charge density difference resulting upon adsorption

We shall examine now in some detail the spatial electronic distribution of the system studied in this work.

In Figs. 7 and 8 we display the charge density difference, i.e., the difference between the density of the adsorption system and its constituents (adlayer and substrate):

$$\Delta n(r) = n_{Pt-OH} - n_{Pt} - n_{OH} \quad (5)$$

The plots are cut along different planes of the system. The blue colour represents the electron deficit regions, while the electron excess regions are coloured in red (i.e., charge flows from blue to red regions). Firstly, these figures distinctly demonstrate the complex interplay between the different orbitals of metal and adlayer. Fig. 7a shows the plane containing the OH axis and the central metal row where it is adsorbed. The increased accumulation of the

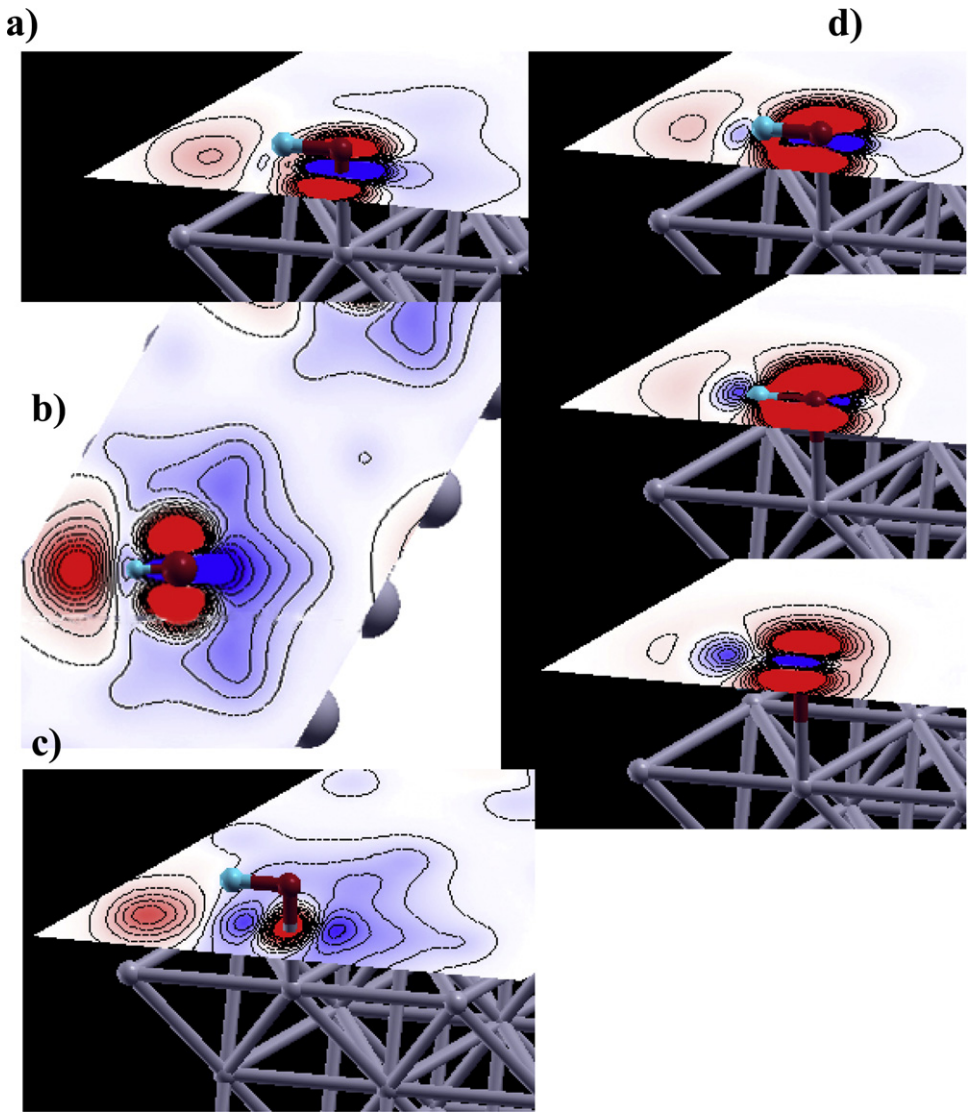

Fig. 8. Different slices perpendicular to the adsorbate–substrate bond and parallel to the O—H bond. (For interpretation of the references to colour in the text, the reader is referred to the web version of the article.)

charge in the region between the oxygen atom and the substrate (red regions located at the middle of the bond) is an indication of chemical bonding. Above and below this middle point of the bond, a depletion of electronic charges is observed, coincident with the decrease in the population of the $2p_0$ and $5d_0$ states. Thus, σ type bonding and antibonding bonds are formed. The split of these states and the shift of the antibonding part above the Fermi level produce this effect (compare Figs. 4 and 6). In contrast, an increase of the electronic charge is observed in the spatial region of the $5d_{\pm1}$, although the changes in the density of these states are not appreciable. Interesting are also the modifications of the electronic density on the neighbouring platinum atoms, especially the region near the hydrogen of the hydroxyl which appreciably increases their charges, while those of the atoms at the other side decreases. Fig. 7b shows a cut in the plane perpendicular to the OH bond. Here, the increase of electronic charge on the oxygen atom is marked, coincident with the increase of the $2p_{-1}$ and $5d_{-1}$ states. Thus, π type bonding and antibonding bonds are formed between these orbitals, which cause the split and shift of these electronic states. However, contrary to the σ type bonds mentioned above, the antibonding part becomes more populated, destabilizing the bond. Like in (a), the decrease in the region of p_0 states is also evident. Fig. 7c shows the charge difference in the top layer of the platinum slab. Particularly on the atom bonded to the oxygen, but also on their neighbours a decrease of the electronic charge is evident. However, an asymmetry is observed in the line of the OH bond. Fig. 7d and e shows that the second layer of the platinum slab is also affected, but in the opposite way: the charge increases on the $5d_0$ and $5d_{\pm2}$ and decrease on the $5d_{\pm1}$ states. Fig. 8 shows different slices perpendicular to the adsorbate–substrate bond and parallel to the O—H bond. These images show that the electronic charge mainly flows to the oxygen atom.

The analysis performed above allows to understand the interaction between the OH layer and the platinum surface when the distance between the adsorbed OH species is enough large such that the formation of hydrogen bond cannot take place. For larger coverage the interaction between neighbour species makes the analysis more difficult. Seitsonen et al. [21] have also performed calculation of charge differences and shown that the hydrogen bonding between OH groups on Pt(1 1 1) and that between water molecules is identical. They described the interaction-induced polarization within the OH group by a gain of electron density in one of the lone-pair orbitals and depletion in the electron density at the H end. They considered that this polarization pattern promotes the

electrostatic attraction between the hydrogen atom and the lone–pair orbital of the adjacent OH group.

4. Conclusions

We have shown a complete overview of the electronic changes produced by the adsorption of hydroxyl on Pt(1 1 1) surfaces at low coverage. A detailed analysis of potential distribution, charge rearrangement, work function changes and distribution of the density of states projected onto the different components and atoms involved in the interaction has been performed. Good agreement with experimental data in the change of the work function upon adsorption of OH has been found. A complicated interplay between the different electronic states takes play. The interaction of the hydroxyl layer with the platinum substrate occurs through all electronic states and all of them participate in the formation of bonds. An interband electronic charge flow occurs between 5d and 6sp states of platinum. Strong changes in the distribution of electronic states of platinum are observed. σ and π molecular states between oxygen and platinum can be identified. The antibonding of the latter lies below the Fermi level, in consequence this bond is less stable than the σ type bonds, where the antibonding part is shifted above the Fermi level.

Acknowledgments

This work is part of the research network financed by the Deutsche Forschungsgemeinschaft FOR1376. The content has been presented and discussed in the internal meeting of ELCAT (Networks of the European Union). P.Q. acknowledges financial support by PICT-2008-0737 (ANPCyT). E.S. acknowledges financial support by PIP-CONICET 112-201001-00411. We thank CONICET (Argentina) for continued support. Finally, fruitfully discussions with Prof. W. Schmickler are gratefully acknowledged.

References

[1] N. Markovic, H. Gasteiger, P.N. Ross, Journal of the Electrochemical Society 144 (1997) 1591.
[2] A. Yamakata, T. Ishibashi, H. Onishi, Journal of Molecular Catalysis A: Chemical 199 (2003) 85.
[3] C. Bianchini, P.K. Shen, Chemical Reviews 109 (2009) 4183.
[4] See for example: E. Santos, W. Schmickler (Eds.), Catalysis in Electrochemistry: From Fundamentals to Strategies for Fuel Cell Development, Wiley, Singapore, 2011.
[5] P.B. Balbuena, D. Altomare, N. Vadlamani, S. Bingi, L.A. Agapito, J.M. Seminario, The Journal of Physical Chemistry A 108 (2004) 6378.
[6] G.S. Karlberg, Physical Review B 74 (2006) 153414.
[7] A. Michaelides, P. Hu, Journal of Chemical Physics 114 (2001) 513.
[8] Y.W. Huang, T.Y. Chou, G.Y. Yu, S.L. Lee, Journal of Physical Chemistry C 115 (2011) 9105.
[9] C. Clay, A. Hodgson, Current Opinion in Solid State & Materials Science 9 (2005) 11.
[10] T. Schiros, L.Å. Näslund, K. Andersson, J. Gyllenpalm, G.S. Karlberg, M. Odelius, H. Ogasawara, L.G.M. Pettersson, A. Nilsson, Journal of Physical Chemistry C 111 (2007) 15003.
[11] G.B. Fisher, B.A. Sexton, Physical Review Letters 44 (1980) 683.
[12] A. Hodgson, S. Haq, Surface Science Reports 64 (2009) 381.
[13] H. Ogasawara, B. Brena, D. Nordlund, M. Nyberg, A. Pelmenschikov, L.G.M. Pettersson, A. Nilsson, Physical Review Letters 89 (2002) 276102.
[14] A. Michaekides, Applied Physics A 85 (2006) 415.
[15] Y. Gohda, S. Schnur, A. Gross, Faraday Discussions 140 (2009) 233.
[16] S. Stolbov, T.S. Rahmanm, Physical Review Letters 89 (2002) 116101.
[17] M.T.M. Koper, Electrochimica Acta 56 (2011) 10645.
[18] Ch.D. Taylor, R.G. Kelly, M. Neurock, Journal of the Electrochemical Society 154 (2007) F217.
[19] M. Chen, S.P. Bates, R.A. van Santen, C.M. Friend, Journal of Physical Chemistry B 101 (1997) 10051.
[20] H. Xin, S. Linic, Journal of Chemical Physics 132 (2010) 221101.
[21] A.P. Seitsonen, Y. Zhu, K. Bedürftig, H. Over, Journal of the American Chemical Society 123 (2001) 7347.
[22] B. Santra, A. Michaelides, M. Fuchs, A. Tkatchenko, C. Filippi, M. Scheffler, Journal of Chemical Physics 129 (2008) 194111.
[23] A.K. Keikkanen, B.I. Lundqvist, J.K. Nørskov, Journal of Chemical Physics 131 (2009) 046102.
[24] Ch. Stoffelsma, P. Rodriguez, G. Garcia, N. Garcia-Araez, D. Strmcnik, N.M. Markovic, M.T.M. Koper, Journal of the American Chemical Society 132 (2010) 16127.
[25] B. Hammer, J.K. Nørskov, Surface Science 343 (1995) 211.
[26] E. Santos, W. Schmickler, Chemical Physics 332 (2007) 39.
[27] E. Santos, W. Schmickler, Angewandte Chemie International Edition 46 (2007) 1.
[28] E. Santos, A. Lundin, K. Pötting, P. Quaino, W. Schmickler, Physical Review B 79 (2009) 235436.
[29] B. Hammer, L.B. Hansen, J.K. Nørskov, Physical Review Letters 59 (1996) 7413, www.fysik.dtu.dk/campos.
[30] D. Vanderbilt, Physical Review B 41 (1990) 7892.
[31] J.P. Perdew, K. Burke, M. Ernzerhof, Physical Review Letters 77 (1996) 3865.
[32] H.J. Monkhorst, J.D. Pack, Physical Review B 13 (1976) 5188.
[33] L. Bengtsson, Physical Review B 59 (1999) 12301.
[34] A. Kokalj, Computational Materials Science 28 (2003) 155 (code available from http://www.xcrysden.org/).
[35] A.B. Anderson, N.M. Neshev, R.A. Sidik, P. Shiller, Electrochimica Acta 47 (2002) 2999.
[36] G. Heimel, L. Romaner, J.L. Brédas, E. Zojer, Physical Review Letters 96 (2006) 196806.
[37] G. Heimel, L. Romaner, E. Zojer, J.L. Brédas, Nano Letters 7 (2007) 932.
[38] G.M. Rangger, L. Romaner, G. Heimel, E. Zojer, Surface and Interface Analysis 40 (2008) 371.
[39] A. Gross, S. Schnur, in: E. Santos, W. Schmickler (Eds.), Catalysis in Electrochemistry: From Fundamentals to Strategies for Fuel Cell Development, Wiley, Singapore, 2011 (Ch. 5).
[40] C. Nyberg, C.G. Tengstal, Journal of Chemical Physics 80 (1984) 3463.